Annals of Biomedical Research
An open access journal
eSciRes
ABR-2-114
Mini Review

Atomistic Simulation Analyses of Sequence-nonspecific Effects of Lipid Composition on Transmembrane Helical Peptide Dimerization

Nishizawa K* and Nishizawa M
School of Medical Technology, Teikyo University, Japan

Abstract

For the dimerization/multimerization of transmembrane (TM) proteins, specific peptide motifs mediate the interactions between transmembrane domains (TMDs). However, the sequence-nonspecific interactions among TMDs as well as between TMDs and lipids may also be important in determining the basal propensities for the association of TM proteins. For this, experimental and computational analyses using model peptides with simple amino acid sequences have been previously used. Recently, we performed an extensive set of united-atom (totaling ~1300 μs) and all-atom simulations (~200 μs), mainly computing free energy for the dimerization of TM model peptides. In this mini-review, we discuss our findings on the sequence-nonspecific effects of lipids on the dimerization of TM helical peptides. An increase in cholesterol in the membranes stiffens the membranes and stabilizes the dimeric state of the TM helical peptides. Cholesterol increased the order parameter of the phospholipid acyl chains and, intriguingly, increased the number of the chains in contact with both peptides, resulting in the better solvation of the peptides in the dimeric state. In contrast, in cholesterol-free phospholipids bilayers, the monomeric state was stabilized because the good coordination of the lipid headgroup atoms with the peptides lowered the electrostatic potential energy. Our analysis also demonstrated the limited parameter transferability of the united-atom force-fields, which caused erroneous results in the simulation analyses of the TMD associations.

Importance of loose and dynamic association between TM helical peptides

Dimerization is a common mechanism for the activation of many single-spanning TM protein receptors [1]. As such, helical TM domains (TMDs) are known to play an important role in dimerization. In cases where cellular receptors for cytokines and hormones for cellular signaling are important, such TMD-TMD interactions are often considered dynamic [1]. For example, recent studies of receptor tyrosine kinases have underscored the importance of the dynamic associations of TM helices [2]. For several hormone and cytokine receptors, multiple steps of interactions are considered to be important for activation by the ligands. Some receptors are known to reside in a state of inactive dimers, and ligands can induce dynamic associations between TMDs which in turn trigger cellular signal transduction. For example, the regulation of vascular endothelial growth factor receptor (VEGFR)-2 activity is explained by the pre-formed dimer model, in which the presence of inactive dimers and subsequent ligand-induced structural changes are considered important for its activation [3].

Such a dynamic type of interaction is likely to be enabled by the fine tuning of the force acting between the TM helices as well as by the loose association between the TM helices, which is most likely mediated by van der Waals interactions rather than by electrostatic interactions between polar residues [1]. Unlike the amino acids with small side chains (SCs), such as Gly, Ala, and Ser, the branched-chain amino acids (Val, Leu, and Ile) act to limit the access of peptide backbones to each other, thus enabling a loose association between TMDs. Intriguingly, the proportion of the branched-chain amino acid contained in the TMDs of disease-related single-pass proteins listed in Moore et al. [1] was significantly higher than those in the TMDs of a wider range of membrane proteins (168 families) compiled by Liu et al. [4]; Val, Leu, and Ile accounted for 51% of the amino acids comprising the TMDs in Moore et al. [1], which was greater than the 34% found by Liu et al. [4] ($p<10^{-10}$) as we discussed [5]. This is consistent with the view that Val, Leu, and Ile enable moderately loose and dynamic interactions that are useful for signal transduction.

Different fatty acids (FAs) are known to exert distinct effects on cellular activities [6-8]. Although specific FA and protein interactions are known to regulate cellular activity, as in the case with GPR120, a receptor for n-3 FA [9], it is plausible that the dynamics of the TMD-TMD interactions are under modulation by the FA composition of the membrane phospholipids [2] and, in particular, the indirect effects of FAs through the modification of the physicochemical properties of the membranes, including the formation of lipid-mediated microdomains, which may play important roles in TMD-TMD interactions [10,11]. In addition, for cholesterol, although specific cholesterol recognition by peptide motifs such as the CRAC (cholesterol recognition/interaction amino acid consensus sequence) motif is well known [12], cholesterol can exert its action through cholesterol-phospholipid interactions. It is known that cell stimulations cause the cholesterol- and sphingolipid-rich microdomains of the plasma membrane to merge into larger platforms, facilitating the interactions of some receptors with their signaling molecules [13,14]. In general, lipid rafts have been suggested to promote clustering of membrane proteins which can also dissociate from each other when located outside of the lipid raft or when the lipid

rafts are dispersed. It is plausible that such microdomains with higher levels of acyl chain order may have some structural advantage in promoting TMD-TMD dimerization compared to more fluidic phospholipid bilayers.

In vitro peptide dimerization assays as well as MD simulations have been used in the study of TMD interactions [15]. Thus far, computational studies of TMD interactions have mainly focused on specific sequences or polar/charged amino acid residues mediating TMD interactions. To name but a few recent studies, Arkhipov et al. [16] showed that TM helices of epidermal growth factor receptor (EGFR) can dimerize near their N or C termini, which were later implicated in the active and inactive dimers of this receptor, respectively [16]. The dimerization of glycophorin A (GpA) TMD has been extensively analyzed by MD simulations (e.g., [17,18]), and some studies have used atomistic simulations to measure the dimerization free energy [19-22] as we discuss later. On the other hand, both experimental and simulation-based analyses of the model peptides with simple amino acids sequences have been limited. Using an *in vitro* system, Mall et al. [23] examined the effects of phospholipids carrying different acyl chains on the dimerization free energies of Lys-flanked Leu-rich TM helical peptides. Matsuzaki and coworkers [24] demonstrated that the addition of cholesterol stabilized the dimeric state of the $(AALALAA)_3$ peptide using liposomes composed of palmitoyloleoylphosphatidylcholine (POPC). To our knowledge, however, there are only a few MD simulation-based measurements of dimerization energy for model peptides. Castillo et al. [25] reported the coarse-grain simulation-based free energy analysis of model peptides known as WALP (Trp-flanked poly-(Leu-Ala) stretch of variable length) peptides. Atomistic simulation-based analyses of the model peptide dimerization energy have most likely been limited due to the computational burden.

Raft-like bilayers assist self-association of TM helical peptides in a sequence–nonspecific manner

We recently conducted an extensive set of united-atom (UA) and all-atom (AA) simulations for the measurement of the free energy of the dimerization of several TM helical peptides. As UA force-fields (FFs), we used the GROMOS 53a6 (Gr^{53a6}) [26,27] and, in earlier studies, OPLS-all atom FF (protein) in combination with Berger lipids (OPLS/Berger or OB) [28,29]. For select analyses we also used Charmm united-atom FF (Ch^{UA}) [30]. For AA FF, we used Charmm 36 (Ch^{36AA}) [31,32]. The dimerization energy was derived from the two-dimensional radial distribution function (rdf) profile, which was computed from the potential of mean field (PMF) profile [5,33]. The umbrella sampling method was used to compute the PMF profile. As the lipid bilayer membranes, we mainly used a DOPC bilayer and 1:1:1 and 2:1:1 dipalmitoylphosphatidylcholine (DPPC)/POPC/cholesterol bilayers. The latter two bilayers showed a high acyl chain order, forming a liquid-ordered (L_o) phase (Figure 2 of [34]), similar to that reported by Niemela et al. [35].

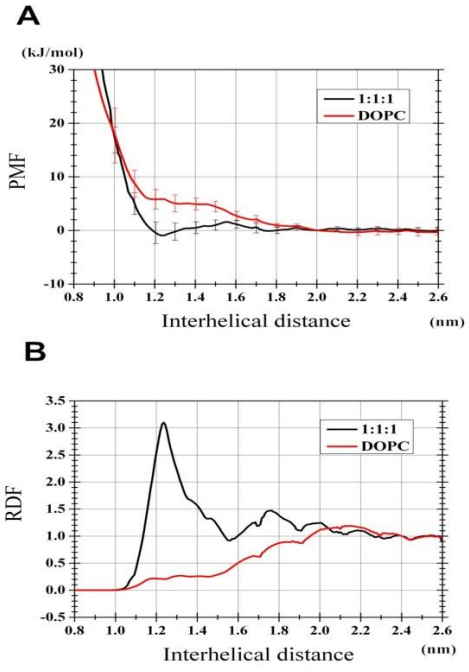

Figure 1: Free energy analysis of Ile21 peptide dimerization in the DOPC and 1:1:1 raft-like bilayer computed with the Gr^{53a6}. (A) The PMF profiles. (B) The rdf profiles derived from the PMF profile.

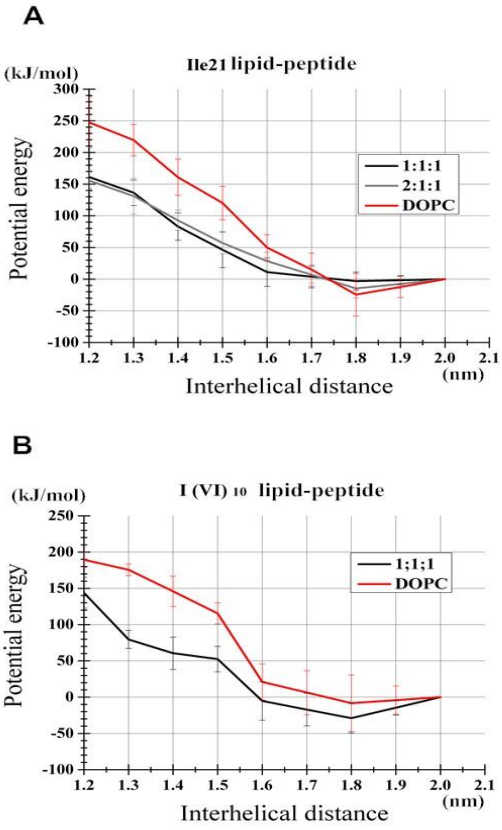

Figure 2: The lipid-peptide potential energy profile $V_{lipid\text{-}pept}$ (r). The value relative to that at the interhelical distance of 2.0 nm is plotted. (A) Ile21. (B) $I(VI)_{10}$.

We henceforth refer to the 1:1:1 and 2:1:1 bilayers as the raft-like bilayers, and the DOPC bilayer as the non-raft bilayer.

Figure 1 shows the representative PMF profiles (with S.E.) and the rdf profiles derived from the PMF profiles of the Gr^{53a6} simulations of the two TM helical Ile21 peptides embedded in the raft-like and non-raft bilayers. These show that the Ile21 dimerization was more favorable in the raft-like bilayer than in the non-raft bilayer. This particular data set was published [34], but we extended the range of the umbrella sampling to 2.5 nm. Table 1 summarizes the dimerization free energy of several peptides reported in our recent studies, along with our new data on $(AALALAA)_3$ peptides and the experimental results. Consistent with the experiments by Yano et al. [24], the simulations with all the model peptides showed a dimer-stabilizing effect for the raft-like bilayers relative to the non-raft bilayers.

To improve the statistical convergence, eight independent runs starting from different initial structures were performed to obtain the S.E. We acknowledge however that, to reduce the computational burden, the range of the distance r between the TM peptides in our PMF analyses had to be limited, typically to 2.0 nm (Figure 1).

Force field	Peptides †	Membrane composition and dimerization energy (kJ/mol)		
Gr^{53a6}	Ile21	DOPC	POPC	1:1:1 DPPC/POPC/cholesterol
		0.23 ± 0.56	-0.06 ± 0.69	-1.34 ± 0.44
Ch^{36AA*}	Ile21	DOPC		1:1:1 DPPC/POPC/cholesterol
		-1.75 ± 0.22		-2.99 ± 0.30
Gr^{53a6}	Ile21	POPC		3:1 POPC/cholesterol
		-0.06 ± 0.69		-0.17 ± 0.75
Gr^{53a6}	$I(VI)_{10}$	DOPC		1:1:1 DPPC/POPC/cholesterol
		0.42 ± 0.59		-1.81 ± 0.57
Gr^{09*}	$(AALALAA)_3$	DOPC		1:1:1 DPPC/POPC/cholesterol
		-9.86 ± 1.79		-13.89 ± 1.21
experiment [2)]	$(AALALAA)_3$	POPC		7:3 POPC/cholesterol
		-13.2		-22.6

*Due to the computational burden, we have computed only for the distances up to 1.6 nm for the Ch^{36AA} and the Gr^{09} sets. †The sequences of the peptides: Ile21, a stretch of 21 residues of Ile; $I(VI)_{10}$, IVIVIVIVIVIVIVIVIVI; $(AALALAA)_3$, AALALAAAALALAAAALALAA. [1)]The results on Ile21 and $I(VI)_{10}$ sets were from ref [34]. The result on Gr^{09}/$(AALALAA)_3$ sets is newly presented here. [2)]Yano et al. [24].

Table 1: Model peptides and dimerization free energy measured by simulations and experiments[1)].

In the case of AA analyses, we had to limit the range down from 0.9 to 1.6 nm. While the rdf curve derived from the PMF profile was basically flat, the range 2.0-2.5 nm and the extension to even longer distances is unlikely to affect the conclusion of these studies, with a possible bias arising from this issue to be critically addressed in the future study.

Another technical issue was that, for the Leu- and Ala-rich sequences, the dimeric state tends to be destabilized under UA FFs, which will be discussed below. As such, instead of Gr^{53a6}, we used the modified version of Gr^{09}, in which the ε parameters of the Lennard-Jones (LJ) potential between the lipid atoms and peptide atoms were rescaled by a factor 0.9, for the $(AALALAA)_3$ peptides in Table 1 using the procedure we recently reported [33,36].

Importantly, for all three peptides tested (Ile21, $I(VI)_{10}$, and $(AALALAA)_3$) the lipid raft-like bilayer (i.e., 1:1:1 DPPC/POPC/cholesterol) stabilized the dimeric state of the peptides compared to the non-raft type bilayers (DOPC, POPC). This is consistent with the experimental results by Yano et al. [24] (bottom of the Table 1). The effect of the cholesterol addition on the dimerization energy appears small compared to the results reported by [24]. The cause for the relatively small effect of cholesterol in the simulations compared to the experiment is presently not clear, but it is possible that the FF inaccuracy accounts for at least a part of the cause; even AA FFs could be inaccurate to describe the effects of the cholesterol addition. Another possibility is that we set the cut-off that discriminates the dimeric state from the monomeric state at 1.6 nm, which may be narrower than in the experiment.

In any event, our computation supported the view that cholesterol and saturated FA acyl chains in the lipid bilayers stabilize the dimerized state of peptides in a sequence-nonspecific manner.

The cholesterol-dependent stabilization of the dimeric state of the helical peptides is driven by the lipid-peptide potential energy term

Next, we investigated the features of the raft-like bilayers stabilized by the peptide dimers in our simulations. Our peptides/raft-like membrane system did not show any sign of spontaneous demixing of lipids into the L_o and liquid-disordered (L_d) domains, however, we observed local-scale (<1 nm scale) inhomogeneity. To be specific, our rdf analysis showed that the TM peptides were in direct contact with phospholipids (under the criteria of residing <2.4 Å from the nearest peptides atoms), whereas cholesterols were preferentially associated with DPPC/POPC but not with the peptides [34]. This can be explained by the well-known structural fitness of cholesterol to phospholipids that favors the positioning of cholesterol in between two or more phospholipid molecules.

Such local inhomogeneity led us to initially hypothesize the 'exclusion (segregation)-based model'; under this model, the peptides dimer is stabilized in the raft-like bilayer by the exclusion of peptides from cholesterol-rich subareas due to the tight interactions between cholesterol and phospholipids. As will be discussed below, however, this hypothesis was not supported by our analysis. Nonetheless, this consideration led us toward a quantitative analysis using decomposition of the potential energy.

Prior to the discussion of our decomposition analysis, it seems beneficial to be reminded of the thermodynamics related to peptide dimerization. The free energy change ΔG_{dim} upon the transition from the monomeric to the dimeric state is decomposed into enthalpy and entropy changes, $\Delta G_{dim} = \Delta H_{dim} - T\Delta S_{dim}$ [25]. In our case, the enthalpy change ΔH is further decomposed into ΔU and the pressure-volume term, where U is the total internal energy (the sum of the kinetic and potential energies). However, the pressure-volume term is usually small and, therefore, ΔH can be considered largely attributable to the change in the total internal energy term ΔU, which in turn parallels the total potential energy term ΔV under constant temperature simulations [25]. As such, $\Delta H_{dim} \fallingdotseq \Delta V_{dim}$, where ΔV_{dim} is the potential energy change upon peptide dimerization. ΔV_{dim} can be more specifically denoted as $\Delta V^{LJ+Coul}{}_{dim}$, where 'LJ+Coul' explicitly denotes the LJ and Coulombic potential energies for clarity.

In Yano et al. [24], the addition of cholesterol to the POPC bilayer caused a shift of the monomer-dimer equilibrium toward the dimeric state; at 298 K, the dimerization free energy ΔG_{dim} of $(AALALAA)_3$ was changed from −13.2 (POPC bilayer) to −22.6 kJ/mol (7:3 POPC:cholesterol bilayer). Yano et al. [24] further showed that the dimerization of the peptide in the POPC bilayer is an enthalpy-driven process and that entropy does not contribute to the dimerization (ΔG_{dim} = –13.2 kJ/mol, ΔH_{dim} = –23.7 kJ/mol, and $-T\Delta S_{dim}$ = 10.4 kJ/mol). Of note, the finding that entropy works against dimerization could be considered as a classical case of mixing entropy. They further showed that the addition of cholesterol to the POPC bilayer increased the unsigned value of ΔG_{dim} and ΔH_{dim}, thus stabilizing the peptide dimerization (ΔG_{dim} = –22.6 kJ/mol, ΔH_{dim} = –84.1 kJ/mol, and $-T\Delta S_{dim}$ = 61.4 kJ/mol) [24]. Thus, the addition of cholesterol increased the enthalpy differential ΔH between the monomeric and dimeric states in the system used by Yano et al. [24]. In contrast, the entropy change $-T\Delta S$ was inhibitory to dimerization and was even more so in the presence of cholesterol. Thus, the enthalpy change but not the entropy change contributed to the cholesterol-induced stabilization of the dimer in the experiment.

To gain an insight into the mechanisms for the raft-like bilayer-dependent stabilization of the peptide dimer, we performed a decomposition analysis of the potential energy V. As the peptides used were not flanked by polar residues, our approach followed that reported by Tieleman and coworkers in their CG analysis [25]; we focused on the three potential energy terms for the lipid-lipid, peptide-peptide, and lipid-peptide interactions, namely, $V_{lipid\text{-}lipid}$, $V_{pep\text{-}pept}$, and $V_{lipid\text{-}pept}$, that most likely have an influence on TM dimerization [25]. Of note, cholesterol was included in the lipid-lipid interactions. Our initial hypothesis postulated the 'exclusion (segregation)-based model' in which raft-like bilayers generally have stronger lipid-lipid interactions, and that tight lipid-lipid interactions promote the exclusion (segregation) of peptides from lipids, assisting in peptide dimerization. If this model is the case, the change of $V_{lipid\text{-}lipid}$ upon the dimerization should be consistent with this idea. Given that peptide dimerization naturally promotes the detachment of some lipid molecules from the peptides and allows such lipids to form new contacts with other lipids, the $V_{lipid\text{-}lipid}$ potential was expected to drop (change to a more negative value) upon dimerization, which was what happened. However, the raft-like bilayer showed a similar to or a rather smaller magnitude of the decrease in this term compared to the non-raft bilayer, arguing against the contribution of this term to the cholesterol-induced stabilization of the peptide dimer (Figure 5 of [34]). Thus, the exclusion-based scenario was not supported by our analysis.

We also considered the possibility that the peptide-peptide potential energy is a key factor. However, this was also unlikely, as the change of $V_{pept\text{-}pept}$ upon dimerization was comparable between DOPC and the raft-like bilayer (Figure 5 of [34]).

For both peptides to which the decomposition was applied (Ile21 and $I(VI)_{10}$), the $V_{lipid\text{-}pept}$ profile increased upon dimerization (Figure 2). This was not surprising since dimerization inevitably hides the peptides from the lipids and therefore hampers lipid-peptide interactions (reflected by the increased $V_{lipid\text{-}pept}$). Interestingly, this increase (cost) of $V_{lipid\text{-}pept}$ upon dimerization was relatively smaller for the raft-like bilayer system compared to the non-raft bilayer (Figure 2 of [34]). This finding supports the solvation-based model, where peptides in monomeric and dimeric states are solvated by phospholipids to degrees differing between the raft-like and non-raft membranes.

Our analysis further demonstrated that both the electrostatic and LJ components of $V_{lipid\text{-}pept}$, that is, $V^{Coul}{}_{lipid\text{-}pept}$ and $V^{LJ}{}_{lipid\text{-}pept}$, showed changes upon dimerization in favor of the raft-like bilayer-dependent stabilization of the peptide dimer. For example, Table 2 shows the changes in $V^{Coul}{}_{lipid\text{-}pept}$

upon Ile21 dimerization. This demonstrates that the cost (i.e., the increase of $V^{Coul}_{lipid\text{-}pept}$ upon dimerization) is not as large for the raft-like bilayer as in the DOPC bilayer. Thus, the raft-like bilayer helps to reduce the cost for dimerization through this term.

		Gr^{53a6}		Ch^{36AA}	
		DOPC	**1:1:1**	**DOPC**	**1:1:1**
$\Delta V^{Coul}_{lipid\text{-}pept}$ upon dimerization ± S.E. (kJ/mol)[1)]		83.3 ± 13.4	17.4 ± 18.6	-5.2 ± 6.5	-37.5 ± 7.0
$S_{choline}$ ± S.D. [2)]	monomer[1)]	607.2 ± 97.3	470.4 ± 65.5	234.7 ± 74.6	212.4 ± 68.1
	dimer[1)]	464.2 ± 82.3	426.2 ± 71.4	227.9 ± 82.3	219.2 ± 71.2

[1)]The structures from the simulations with r=1.3 and 2.0 nm (for the Ch^{36AA} set, 1.6 nm) were taken as the monomeric and dimeric states, respectively. The differential $\Delta V^{Coul}_{lipid\text{-}pept}$ was derived from the mean $V^{Coul}_{lipid\text{-}pept}$ values. [2)]To represent the range of fluctuations, S.D. is shown instead of S.E.

Table 2: Differences between DOPC and the raft-like bilayer in lipid-peptide electrostatic potential energy and the proximity index $S_{choline}$: An example from the Ile21 dimerization analysis [37].

Interactions between TM peptides and lipid headgroups for dimer-stabilization in the lipid raft-like bilayer

Next, we addressed the issue of the structural basis for which the lipid-peptide electrostatic potential energy $V^{Coul}_{lipid\text{-}pept}$ has an important role in the dimer stabilization of raft-like bilayers. As the lipid acyl chains and SCs of Val, Leu, Ile, and Ala have no (under Gr^{53a6}) or little (Ch^{36AA}) atomic charges, $V^{Coul}_{lipid\text{-}pept}$ essentially arises from the interactions between the lipid headgroups and the peptide backbones. As such, we further decomposed $V^{Coul}_{lipid\text{-}pept}$ into $V^{Coul}_{choline\text{-}pept}$, $V^{Coul}_{po4\text{-}pept}$, and $V^{Coul}_{glycco\text{-}pept}$, that is, the electrostatic potential energies between the peptide backbone atoms and each choline group, phosphate group, and glycerol backbone of the phosphatidylcholine headgroups, respectively (the 'glycco' of $V^{Coul}_{glycco\text{-}pept}$ stands for 'the glycerol backbone plus carbonyl oxygen'). Intriguingly, the $V^{Coul}_{choline\text{-}pept}$ and $V^{Coul}_{glycco\text{-}pept}$ profiles showed a decrease upon peptide dimerization, implying that these factors contribute to the stabilization of the monomeric state in the DOPC bilayer (Figure 3 of [37]). In contrast, in the analyses with the raft-like bilayer, these components showed largely flat profiles, suggesting no or little impact by these factors on the monomer-dimer equilibrium of the raft-like bilayer (Figure 3 of [37]).

To determine why the choline-peptide electrostatic energy $V^{Coul}_{choline\text{-}pept}$ decreases (that is, become energetically favored) when the peptides are monomerized in the DOPC bilayer, a structural account for this monomer-stabilizing property of the $V^{Coul}_{lipid\text{-}pept}$ in the DOPC simulations was carried out using a so-called proximity index analysis. Here, we use the word 'proximity' to distinguish from 'contact', which we used for the coordination analysis of the LJ interactions. Our proximity analysis is similar to the usual coordination analysis, however, given the long-range nature of electrostatic interactions, we determined the coordination within a relatively wide range. Specifically, we chose to compute the sum $S_{choline}$ of N_{bb8} over all atoms of the choline group, where N_{bb8} denotes the number of peptide backbone atoms located within 8 Å of the (reference) atom of the lipid molecule. Of note, while N_{bb8} represents the number of the peptide backbone atoms located in vicinity, $S_{choline}$ represents the number of the 'pairs' between a choline atom and a peptide backbone atom located in vicinity. As the lower half of Table 2 shows, $S_{choline}$ was 607.2 for the Ile21/DOPC system with an interhelical distance r=2.0 nm (monomeric state), significantly higher than 464.2 with r=1.3 nm (dimeric state) (Table 2). Thus, in the Ile21/DOPC system, the monomeric peptides have more atoms, in their proximity, from the lipid headgroups, compared to the peptides in the dimeric state. When the same analysis was done for the glycerol backbone of DOPC, the sum S_{glycco} of N_{bb8} also showed a similar dimer-*vs.*-monomer difference in the DOPC simulations (1162 *vs.* 950), indicating the presence of more lipid headgroup atoms in proximity of the peptides in monomers relative to dimers. This is a better fit for the DOPC headgroups to the peptides in the monomeric state in DOPC bilayers, stabilizing the monomeric state (Figure 3A). In contrast, in the 1:1:1 raft-like bilayer, $S_{choline}$ showed only a small difference upon dimerization for the Gr^{53a6} analysis and did not show a better score for the monomeric state in the Ch^{36AA} simulations (Table 2). Similarly, S_{glycco} showed only a modest change upon dimerization for the raft-like bilayer [37]. In the raft-like bilayer system, the cholesterol-phospholipid interactions may restrict the range of motion of the headgroups, thereby compromising the fit of the headgroups to the peptides in the monomeric state compared to the system with the DOPC bilayer.

Taken together, these results show that, unlike the 1:1:1 bilayer, the DOPC bilayer can form better associations between the peptides and lipid head groups when the peptides are in a monomeric rather than dimeric state (Figure 3A). This contributes to the between-membrane difference of the dimerization propensity.

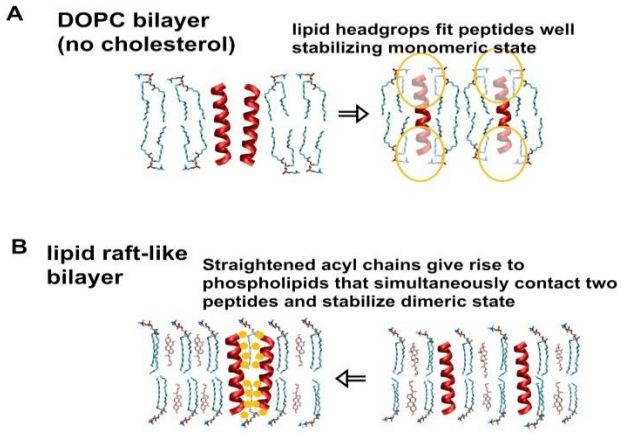

Figure 3: Schematic model representing the structural differences between the non-raft-like DOPC bilayer and the raft-like bilayer relevant to the stability of the dimeric state of the TM peptides. (A) DOPC bilayer. Our analyses showed that the better fitting of lipid headgroups compared to the raft-like bilayer lowers the lipid-peptide electrostatic potential energy thereby stabilizing the monomeric state. (B) Raft-like bilayer. Cholesterol-induced straightening of the acyl chains enables some lipid molecules to contact to two peptides in dimeric state simultaneously (dual contacts), thereby decreasing the LJ potential energy between lipids and peptides.

To evaluate the impact of the lipid headgroup-peptides interactions, we examined the correlation between these proximity indices with $V^{Coul}_{lipid\text{-}pept}$. When the simulation trajectories were divided into short segments (100 ns), the sum of the proximity indices ($S_{choline} + S_{glycco} + S_{po4}$) derived from each trajectory segment exhibited a large between-segment variance and, importantly, showed a significant correlation with the mean $V^{Coul}_{lipid\text{-}pept}$ of the segment (Figure 5 of [37]). These features were observed for both of the peptides examined (i.e., Ile21 and $I(IV)_{10}$). Thus, we concluded that the proximity indices are the metrics describing the structural features, which have strong associations with the changes in electrostatic interaction energy.

Lipid acyl chain coordination to peptides also contributes to the stabilization of the dimer in the raft-like bilayer

In addition to the electrostatic potential energies discussed above, the LJ interactions between the phospholipids and the peptides were found to play an important role in the stabilization of the monomeric state of peptide dimerization. Our decomposition analysis showed that the profile of LJ energy between lipids and peptides is an important factor, contributing to the dimer stabilization of the raft-like bilayer (Figure 6 in [34]). For example, the increase in $V^{LJ}_{lipid\text{-}pept}$ at r=1.3 nm relative to the value at r=2.0 nm represents the cost ascribed to this LJ term. However, the cost for Ile21 dimerization was 119.1 kJ/mol in the raft-like system, which was smaller than the cost of 136.2 kJ/mol in the DOPC system, which supports the view that $V^{LJ}_{lipid\text{-}pept}$ contributes to the cholesterol-dependent stabilization of the dimer (Table 3). A similar trend was observed for $I(VI)_{10}$ under Gr^{53a6} and for Ile21 under Ch^{36AA} [37].

	Gr^{53a6}		Ch^{36AA}	
	DOPC	**1:1:1**	**DOPC**	**1:1:1**
Increase in $V^{LJ}_{lipid\text{-}pept}$ upon dimerization ± S.E. (kJ/mol)	136.2 ± 15.4	119.1 ± 3.9	78.1 ± 8.1	61.8 ± 7.0
Number of C12-C16 atoms with dual contact to dimeric peptides ± S.D.	7.9 ± 3.2	8.5 ± 3.3 ($p<10^{-8}$)*	5.7 ± 3.1	6.9 ± 3.2 ($p<10^{-20}$)*

*p-values are for the comparison between the DOPC and the 1:1:1 bilayer membranes.

Table 3: Increase in the lipid-peptide LJ potential energy $V^{LJ}_{lipid\text{-}pept}$ (kJ/mol) upon dimerization and the number of distal acyl chain segment (C12-C16) atoms that were in contact with both peptides (placed with the interhelical distance r=1.3 nm, i.e., in the dimeric state) simultaneously. Results on the Ile21 peptides analyses are shown.

To determine the structural reason for the smaller energy cost in $V^{LJ}_{lipid\text{-}pept}$ upon dimerization in the raft-like bilayer, we conducted a coordination analysis. We hypothesized that the straightened acyl chains of the raft-like bilayers can come into contact with both of the dimerized peptides simultaneously, such that 'dual contacts' may contribute to the raft-like bilayer-dependent stabilization of the TM peptide dimer. As such, we determine the number ($N_{acyl\text{-}dist}{}^{dual}$) of the acyl chains whose all nine distal carbon atoms (i.e., C9-C16) had dual contacts (within 5 Å) with dimerized peptides (r=1.3 nm), and found that there were more such acyl chains for the raft-like bilayer system relative to the non-raft-type bilayer system (Table 4 of [37]). In fact, $N_{acyl\text{-}dist}{}^{dual}$, (± SD) was 0.089 (± 0.292) for the Ile21/DOPC system, and 0.170 (± 0.408) for the Ile21/1:1:1 bilayer system ($p<10^{-11}$). Similar differences were observed for all the settings examined (i.e., Gr^{53a6} $I(VI)_{10}$ and Ch^{36AA} Ile21 system) as well as with a loosened definition of the dual contact (6 Å cut-off). We then conducted an atom-based analysis and observed consistent results. These findings indicate that the acyl chains come into contact with the two peptides simultaneously and that dual contact is more frequently formed in the raft–like bilayer (Figure 3B) than in the DOPC bilayer. We further analyzed the correlation between the $V^{LJ}_{lipid\text{-}pept}$ and $N_{acyl\text{-}dist}{}^{dual}$ values obtained from the 100 ns segments of the trajectory of dimer-peptide-containing simulations (r=1.3 nm). For all the settings tested, a significant correlation was observed, indicating that the dual contacts have an important impact on the potential energy.

Peptide*	Membrane†	Force field and dimerization energy			Energy from experiment	Reference
KL22	DOPC	Gr^{53a6}	Ch^{UA}	Ch^{36AA}	-8.3	[5,23]
		-1.55 ± 1.00	-3.31± 0.28	-7.46 ± 2.04		
$(AALALAA)_3$	DOPC	Gr^{53a6}	OB	Ch^{36AA}	-12.7	[33,39]
		-5.2 ± 1.0	-4.4 ± 1.4	-9.9 ± 1.3		
L21	DOPC	Gr^{53a6}		Ch^{36AA}	n.d[1)]	[5]
		-0.24 ± 0.80		-6.12 ± 2.00		
A21	oc/diC_4PC	Gr^{53a6}		Ch^{36AA}	n.d[1)]	[5]
		-1.95 ± 0.25		-3.86 ± 0.54		

*For the KL22 set, hetero-dimerization was analyzed. The peptide sequences used are as follows: KL22, KKGLLLLLLLLLLWLLLLLLLLLLLLKKA and KKGLLLLLLLLLLYLLLLLLLLLLLLKKA but 'Y (Tyr)' of the latter peptide was dibromotyrosine in [23]; $(AALALAA)_3$ is given under the Table 1; L21 is a stretch of 21 Leu residues; A21 is a stretch of 21 Ala residues. †DOPC stands for the DOPC bilayer. oc/diC_4PC is octane/ dibutyrylphosphatidylcholine, that is, a bilayer mimetic comprised of an octane slab sandwiched by the dibutyrylphosphatidylcholine layers. 1)n.d. = not determined experimentally to our knowledge.

Table 4: Comparison between UA and AA FFs in dimerization energy (kJ/mol) for Leu- or Ala- rich TM helical peptides.

Technical challenge: Discrepancy between united-atom and all-atom force fields in TM dimerization analyses

Due to the computational burden of the AA and UA simulations of the systems comprised of protein(s)/membrane/water, adequate sampling is often a challenge. An increasing number of MD simulation-based studies on TMD-interactions now utilize procedures that control the axial orientation in order to better cover the association interfaces (e.g., [38]). As our set-up used peptides with simple sequences and lacking specific interfaces for the peptide association, performing many independent simulation mitigated the sampling problem arising from the within-trajectory correlation (specifically, the precision of 0.5 kJ/mol in S.E. for the UA simulation was attainable in about two months, using ~25 Intel core i5 CPU PCs, whereas the use of AA simulations required a 3 to 5-fold greater computation time). We have to emphasize, however, that, rather than the issue of sampling (precision), the issue of inaccuracy that stems from poor transferability of UA FFs is potentially more problematic. As will be considered below, the UA FFs have a limited degree of parameter transferability for systems containing phospholipids-water interfaces. Overall, the precision was reasonably good for our intended purposes, however, the inaccuracy often presented challenges, especially in the cases where UA FFs were used. It should also be added that in some settings AA FFs also show inaccurate estimation of the dimerization energy [22].

In our analyses, the inaccuracy of the UA simulation results was a serious issue. Selected examples demonstrating the AA *vs.* UA discrepancy are shown in Table 4. For example, for the $(AALALAA)_3$ peptide embedded in the DOPC bilayer, OB and Gr^{53a6} showed a dimerization energy of ~-5 kJ/mol, whose unsigned value was much smaller than -9.9 under Ch^{36AA} and -12.7 kJ/mol from the experiment [33,39]. To reduce the computation time, certain analyses were carried out with an octane slab covered by diC_4PC slabs instead of a phospholipids bilayer. For all the Leu-rich and Ala-rich peptides tested, Gr^{53a6} tended to show a higher dimerization tendency relative to Ch^{36AA} simulations. Ch^{UA} showed an intermediate dimerization energy between Gr^{53a6} and Ch^{36AA}. The poly-Val and poly-Ile peptides showed a modest level of discrepancy between Gr^{53a6} and Ch^{36AA} [5].

Our analysis indicated that UA FFs tended to show weak dimerization propensity for Leu- and Ala-rich TM peptides due to the limited transferability of the UA FF parameters. On the other hand, for the amino acid side chain analogues (SCAs) of Val, Leu, Ile, and Phe, Ch^{AA}, Gr^{53a6}, and OB showed a good agreement in terms of solvation energy and dimerization energy in octane [36]. Intriguingly, as the system progressively became more complex and biologically relevant, the UA *vs.* AA discrepancy grew, suggesting the limited parameter transferability of the UA models to the lipid-water interface [36]. In the layer containing the lipid-water interface, lipid headgroup atoms, and the peptide termini, the lipid-peptide interactions may not be represented with sufficient accuracy.

Due to this, care should be taken when UA parameter sets are used for the evaluation of TMD dimerization propensity when TMD-TMD dimerization is relatively weak, as in the case of sequence-nonspecific dimerization. While UA models can be useful for the analysis of high affinity dimerization events in which a specific motif (such as a GXXXG motif) allows for compact TM peptides interactions, our results demonstrate that the UA models may engender erroneous results, especially for Leu- and Ala- rich peptides.

Notably, inaccuracy in representing the water-lipid interface can also be severe for CG models. For example, our analysis using MARTINI CG models [40] showed that, in a dilauroylphosphatidylcholine (DLPC) bilayer, the dimerization PMF profile of the helical peptide with a

sequence 'SGWW$(L)_{13}$WWAS' showed a well with a depth of -16.6 kJ/mol, but 'GGWW$(L)_{13}$WWAG' showed -12.5 kJ/mol [41]. In similar settings, the well depth of the dimerization PMF for 'GWW$(L)_9$WWA' was -20.4 kJ/mol, but that for 'GGWW$(L)_9$WWAG' was -29.7 kJ/mol, despite only one Gly residue being added at both ends. Although the reference simulations under atomistic FFs remain to be done, these findings indicate the high sensitivity of CG analyses to the structure of the water/lipid/TM peptide termini and negative mismatching [41]. This finding supports the difficulty in CG parameterization of peptides placed at lipid-water interfaces [42].

It should also be noted that AA simulations can also lead to erroneous results. Domanski et al. [22] recently showed that computations with the AA FFs including Charmm36 and Amber (protein) in combination with Slipid [43] all showed dimer instability (apparently positive dimerization free energies) for the GpA TM peptide in a POPC bilayer. This is inconsistent with the experimental data that showed dimerization free energy ranging -16 − -51 kJ/mol [44]. Intriguingly, the analysis with an UA model (Gromos 43a2) by Kuznetsov et al. [21] showed a dimerization PMF profile with a well-depth of -60 kJ/mol, which is more consistent with the experiments. This value, along with a couple of CG–based measurement [18,20] suggesting that in this setting UA is closer to the experimental results [21].

Biological and technical perspectives

As has been discussed above, in our MD simulations, the raft-like bilayer consistently exhibited a stabilizing effect on the dimeric state of the TM model helical peptides compared to the DOPC bilayer. The peptides used had simple sequences of hydrophobic amino acids, where some were lacking flanking polar/charged residues. This allowed us to evaluate the sequence-nonspecific effects of lipid membranes on the dimerization propensities.

Despite the lack of charged or polar amino acid residues in the model peptides, the electrostatic interaction between lipid headgroups and peptide backbones was unexpectedly found to influence the monomer-dimer equilibrium. It is possible that the relatively low dielectric coefficient at the layer containing the glycerol backbone and the ester bonds of phosphatidylcholine yields interactions between the peptide backbones and lipid headgroups that have an effect on TM dimerization. It is also possible that the addition of flanking sequences of polar or charged residues, such as Lys and Arg, to the peptide termini have a profound effect on the peptide-lipid potential energy and the dimerization energy of the peptide, possibly intensifying the effects of the lipid composition on the peptide dimerization propensity. This line of analysis is underway by our research group. Although not yet tested, the effects of negatively charged phospholipids such as phosphatidylserine (PS) may modify the peptide dimerization propensities in a sequence-nonspecific manner. Bacterial and eukaryotic cell membranes have overall negative charges [45] and, although less abundant than PC and phosphatidylethanolamine (PE), PS is found at a substantial concentration (12%) in mammalian plasma membranes [46]. The negative charge of biological membranes has a significant impact on the stability of TM helical peptides and are considered to help determine the topology of integral membrane proteins [47]. For example, despite the glycophorin A (GpA) TM exists mostly as a dimer in pure POPC bilayers [48], it remains predominantly monomeric in bleb vesicles derived from mammalian cells. Hong and Bowie [47] further showed that the TM domain of GpA is destabilized in physiological membranes compared to the POPC membrane, and that the electrostatic interaction between negatively charged lipids and the positively charged residues of the TM helix is responsible for their destabilization. If necessary, our systems could be extended to address such issues.

Our findings provide an insight into the importance of the electrostatic interactions between the headgroups and the peptide backbones of TMDs as well as the impact of the cholesterol-mediated straightening of the lipid acyl chains on the lipid-peptides interactions and on peptide dimerization. However, it is not straightforward to extrapolate our findings to biological systems. Firstly, in cellular membranes, the difference between the liquid-ordered (L_o) and the liquid disordered (L_d) phases is much smaller than in synthetic systems [49]. Besides, both domains are abundant in proteins. Furthermore, acylation of proteins plays a crucial role in localizing various proteins into the lipid raft, thereby affecting the microenvironment of each protein molecule. On the other hand, cholesterol exists even outside of the lipid rafts and could impact the structure of acyl chains outside of the lipid rafts. Not only cholesterol but also FAs play roles across distinct microdomains. For example, polyunsaturated FA (PUFA)-treatment of Jurkat T cells led to increased PUFAs in phospholipids not only in bulk membranes but also in isolated lipid rafts and led to the displacement of proteins from lipid rafts [50]. We used the raft-like membrane and DOPC bilayer due to a clear comparison, however, we also used POPC and 3:1 POPC/cholesterol bilayers and observed a small but consistent and essentially similar effect of cholesterol (Figure 4 and 5 of [34]). This supports that cholesterol-induced changes of the membrane structure could have an impact on the TMD dynamics in a wide range of lipid ordering and stiffness. Thus, we surmise that regardless of whether the location of the TM protein is within or outside of the lipid rafts, the cholesterol content and FA content/species could have an impact on the TMD dynamics.

In the following, we would like to make note of a technical issue. Our studies highlighted the interactions between phospholipids and the peptide backbone, in particular through electrostatic forces, as an important factor for determining the dimerization propensities. As such, it is worth noting that UA models and, in some settings, AA models as well have a limited transferability and, in some cases, may yield erroneous results for TMD dynamics, as was noted above. As discussed previously by Tieleman and coworkers, the use of an FF-optimized protein for aqueous environments in combination with a FF prepared for lipid membranes is not straightforward [51]. Our analyses examined this problem and found a situation where the problem worsened; UA models

(even UA FFs, despite being well-studied for both lipids and proteins) can exhibit limited transferability especially in protein/lipid interactions near lipid headgroups, leading to erroneous results. This limited parameter transferability is striking given that, in the analyses with simple systems made up of SCAs and apolar solvents, the UA FFs were in agreement with the Ch^{36AA} results [36].

Despite this drawback, UA models can still be useful for many analyses of lateral association of membrane proteins, given that readjustment of the TMD-TMD association energy is possible using a simple method such as our LJ-rescaling method [33]. With this method, the parameters of the lipids and protein parts of the original FFs are not changed, and only the LJ terms between the lipid and protein atoms (cross-terms) are rescaled. This way, the specific protein-protein and lipid-lipid interactions remain unchanged from the original Gr^{53a6}. The interactions between amino acids and water are also unchanged. Of note, the same procedure as ours was also attempted in Domanski et al. [22] in adjusting the GpA TMD dimerization free energy to the experimental value. From our experience, it is worth checking the dimerization PMF (sometimes a quick check using octane/diC_4PC is sufficient) and, when appropriate, attempting LJ-rescaling so that the TM interaction force becomes similar to those under AA simulation and, when available, the experimental data. Although we used a universal rescaling factor for all the amino acids in the peptides ([36] and Table 1), using distinct rescaling factors for amino acid residues located at different positions of the peptides (e.g., the termini or the central segments) may also be beneficial. For example, it is possible that only a few terminal residues suffer from a wide UA-vs-AA discrepancy, whereas the residues of the central segment show acceptable degrees of such discrepancy. We are currently conducting analyses to address this issue and to develop procedures for the better adjustment of the parameters.

Acknowledgement

The authors would like to thank two anonymous reviewers for their constructive comments.

Compliance with Ethical Standards

Conflict of Interest

Authors declare that they have no conflict of interest.

Ethical approval

This article does not contain any studies with human participants or animals performed by any of the authors.

References

1. Moore DT, Berger BW, DeGrado WF (2008) Protein protein interactions in the membrane: Sequence, structural, and biological motifs. Structure 16(7): 991-1001.

2. Bocharov EV, Mineev KS, Pavlov KV, et al. (2017) Helix-helix interactions in membrane domains of bitopic proteins: Specificity and role of lipid environment. Biochim Biophys Acta 1859(4): 561-576.

3. Sarabipour S (2017) Parallels and distinctions in FGFR, VEGFR, and EGFR mechanisms of transmembrane signaling. Biochemistry 56(25): 3159-3173.

4. Liu Y, Engelman DM, Gerstein M (2002) Genomic analysis of membrane protein families: Abundance and conserved motifs. Genome Biol 3(10): research 0054-1.

5. Nishizawa M, Nishizawa K (2018c) Force-field dependency of Leu-rich helical peptides dimerization energy in lipid bilayers. I. United-atom simulations show discrepancy from experiments and all-atom simulations. Ann Biomed Res 1: 112.

6. Estadella D, da Penha Oller do Nascimento CM, Oyama LM, et al. (2013) Lipotoxicity: effects of dietary saturated and trans fatty acids. Mediators Inflamm.137579.

7. Ruiz-Núñez B, Dijck-Brouwer DA, Muskiet FA (2016) The relation of saturated fatty acids with low-grade inflammation and cardiovascular disease. J Nutr Biochem 36: 1-20.

8. Calder PC (2008) The relationship between the fatty acid composition of immune cells and their function. Prostaglandins Leukot Essent Fatty Acids 79(3-5): 101-108.

9. Oh DY, Talukdar S, Bae EJ, et al. (2010) GPR120 is an omega-3 fatty acid receptor mediating potent anti-inflammatory and insulin-sensitizing effects. Cell 142(5): 687-698.

10. Stulnig TM, Zeyda M (2004) Immunomodulation by polyunsaturated fatty acids: impact on T-cell signaling. Lipids 39(12): 1171-1175.

11. Lorent JH, Levental I (2015) Structural determinants of protein partitioning into ordered membrane domains and lipid rafts. Chem Phys Lipids 192: 23-32.

12. Fantini J, Barrantes FJ (2013) How cholesterol interacts with membrane proteins: an exploration of cholesterol-binding sites including CRAC, CARC, and tilted domains. Front Physiol 4: 31.

13. Lingwood D, Simons K (2010) Lipid rafts as a membrane-organizing principle. Science 327(5961): 46-50.

14. Levental I, Grzybek M, Simons K (2011) Raft domains of variable properties and compositions in plasma membrane vesicles. Proc Natl Acad Sci USA 108(28): 11411-11416.

15. Fink A, Sal-Man N, Gerber D, et al. (2012) Transmembrane domains interactions within the membrane milieu: Principles, advances and challenges. Biochim Biophys Acta-Biomembranes 1818(4): 974-983.

16. Arkhipov A, Shan Y, Das R, et al. (2013) Architecture and membrane interactions of the EGF receptor. Cell 152(3): 557-569.

17. Psachoulia E, Marshall DP, Sansom MS (2009) Molecular dynamics simulations of the dimerization of transmembrane α-helices. Accounts Chem Res 43(3): 388-396.

18. Sengupta D, Marrink SJ (2010) Lipid-mediated interactions tune the association of glycophorin A helix and its disruptive mutants in membranes. Phys Chem Chem Phys 12(40): 12987-12996.

19. Hénin J, Pohorille A, Chipot C (2005) Insights into the recognition and association of transmembrane α-helices. The free energy of α-helix dimerization in glycophorin A. J Am Chem Soc 127(23): 8478-8484.
20. Janosi L, Prakash A, Doxastakis M (2010) Lipid-modulated sequence-specific association of glycophorin A in membranes. Biophys J 99(1): 284-292.
21. Kuznetsov AS, Polyansky AA, Fleck M, et al. (2015) Adaptable lipid matrix promotes protein–protein association in membranes. J Chem Theory Comput 11(9): 4415-4426.
22. Domanski J, Sansom MS, Stansfeld PJ, et al. (2018) Balancing force field protein–lipid interactions to capture transmembrane helix–helix association. J Chem Theory Comput, 14(3): 1706-1715.
23. Mall S, Broadbridge R, Sharma RP, et al. (2001) Self-association of model transmembrane α-helices is modulated by lipid structure. Biochemistry 40(41): 12379-12386
24. Yano Y, Kondo K, Kitani R, et al. (2015) Cholesterol-induced lipophobic interaction between transmembrane helices using ensemble and single molecule fluorescence resonance energy transfer. Biochemistry 54(6): 1371-1379.
25. Castillo N, Monticelli L, Barnoud J, et al. (2013) Free energy of WALP23 dimer association in DMPC, DPPC, and DOPC bilayers. Chem Phys Lipids 169: 95-105.
26. Poger D, Mark AE (2010) On the validation of molecular dynamics simulations of saturated and cis-monounsaturated phosphatidylcholine lipid bilayers: A Comparison with experiment. J Chem Theory Comput 6(1): 325-336.
27. Oostenbrink C, Villa A, Mark AE, et al. (2004) A biomolecular force field based on the free enthalpy of hydration and solvation: The GROMOS force-field parameter sets 53A5 and 53A6. J Comput Chem 25(13): 1656-1676.
28. Berger O, Edholm O, Jähnig F (1997) Molecular dynamics simulations of a fluid bilayer of dipalmitoylphosphatidylcholine at full hydration, constant pressure, and constant temperature. Biophys J 72(5): 2002-2013
29. Jorgensen WL, Maxwell DS, Tirado-Rives J (1996) Development and testing of the OPLS all-atom force field on conformational energetics and properties of organic liquids. J Am Chem Soc 118(45): 11225-11236.
30. Lee S, Tran A, Allsopp M, et al. (2014) CHARMM36 united atom chain model for lipids and surfactants. J Phys Chem B 118(2): 547-556.
31. Huang J, MacKerell Jr AD (2013) CHARMM36 all-atom additive protein force field: Validation based on comparison to NMR data. J Comput Chem 34(25): 2135-2145.
32. Klauda JB, Venable RM, Freites JA, et al. (2010) Update of the CHARMM all-atom additive force field for lipids: Validation on six lipid types. J Phys Chem B 114(23): 7830-7843.
33. Nishizawa M, Nishizawa K (2016) Free energy of helical transmembrane peptide dimerization in OPLS-AA/Berger force field simulations: Inaccuracy and implications for partner-specific Lennard-Jones parameters between peptides and lipids. Mol Simulat 42: 916-926.
34. Nishizawa M, Nishizawa K (2018a) Sequence-nonspecific stabilization of transmembrane helical peptide dimer in lipid raft-like bilayers in atomistic simulations. I. Dimerization free energy and impact of lipid-peptide potential energy. Ann Biomed Res 1: 105.
35. Niemelä PS, Ollila S, Hyvönen MT, et al. (2007) Assessing the nature of lipid raft membranes. PLoS Comput Biol 3(2): e34.
36. Nishizawa M, Nishizawa K (2018d) Force-field dependency of Leu-rich helical peptides dimerization energy in lipid bilayers. II. Limited transferability of united-atom simulation parameters to membrane-water interfaces. Ann Biomed Res 1: 113.
37. Nishizawa M, Nishizawa K (2018b) Sequence-nonspecific stabilization of transmembrane helical peptide dimer in lipid raft-like bilayers in atomistic simulations. II. Acyl chain order-associated changes in lipid-peptide contacts concordant with potential energy profiles. Ann Biomed Res 1: 106.
38. Li PC, Miyashita N, Im W, et al. (2014) Multidimensional umbrella sampling and replica-exchange molecular dynamics simulations for structure prediction of transmembrane helix dimers. J Comput Chem 35(4): 300-308.
39. Yano Y, Matsuzaki K (2006) Measurement of thermodynamic parameters for hydrophobic mismatch 1: self-association of a transmembrane helix. Biochemistry 45(10): 3370-3378.
40. de Jong DH, Singh G, Bennett WFD, et al. (2013) Improved parameters for the Martini coarse-grained protein force field. J Chem Theory Comput 9(1): 687-697.
41. Nishizawa M, Nishizawa K (2014) Potential of mean force analysis of the self-association of leucine-rich transmembrane α-helices: Difference between atomistic and coarse-grained simulations. J Chem Phys 141(7): 075101.
42. Dalgicdir C, Sensoy O, Peter C, et al. (2013) A transferable coarse-grained model for diphenylalanine: How to represent an environment driven conformational transition. J Chem Phys 139(23): 234115.
43. Jämbeck JP, Lyubartsev AP (2012) Derivation and systematic validation of a refined all-atom force field for phosphatidylcholine lipids. J Phys Cem B 116(10): 3164-3179.
44. Hong H, Blois TM, Cao Z, et al. (2010) Method to measure strong protein–protein interactions in lipid bilayers using a steric trap. Proc Natl Acad Sci USA 107(46): 19802-19807.
45. de Kruijff B (1997) Lipid polymorphism and biomembrane function. Curr Opin Chem Biol 1(4): 564-569.
46. Leventis PA, Grinstein S (2010) The distribution and function of phosphatidylserine in cellular membranes. Ann Rev Biophys 39: 407-427.
47. Hong H, Bowie JU (2011) Dramatic destabilization of transmembrane helix interactions by features of natural membrane environments. J Am Chem Soc 33(29): 11389-11398.
48. Chen L, Novicky L, Merzlyakov M, et al. (2010) Measuring the energetics of membrane protein dimerization in mammalian membranes. J Am Chem Soc 132(10): 3628-3635.
49. Kaiser HJ, Lingwood D, Levental I, et al. (2009) Order of lipid phases in model and plasma membranes. Proc Natl Acad Sci USA 106(39): 16645-16650.

50. Stulnig TM, Huber J, Leitinger N, et al. (2001) Polyunsaturated eicosapentaenoic acid displaces proteins from membrane rafts by altering raft lipid composition. J Biol Chem 276(40): 37335-37340.
51. Tieleman DP, MacCallum JL, Ash WL, et al. (2006) Membrane protein simulations with a united-atom lipid and all-atom protein model: Lipid–protein interactions, side chain transfer free energies and model proteins. J Phys Condens Matter 18(28): S1221 -1234.

***Corresponding author:** Kazuhisa Nishizawa, Teikyo University School of Medical Technology, Kaga, Itabashi, Tokyo, 173-8605 Japan, Tel: +81-3-3964-1211, Fax: +81-3-5944-3354; Email: kazunet@med.teikyo-u.ac.jp

Received date: March 22, 2019; **Accepted date:** March 25, 2019; **Published date:** March 26, 2019

Citation: Nishizawa K, Nishizawa M (2019) Atomistic Simulation Analyses of Sequence-nonspecific Effects of Lipid Composition on Transmembrane Helical Peptide Dimerization. *Ann Biomed Res* 2(1): 114.